Supplementary Information

Destruction for Growth: A Novel Laser Direct Writing Perovskite Mechanism with Intelligent Anti-Counterfeiting Applications

Shoufang Liu[a,b#], Xiangyu Xu[a,b#], Jie Zhou[a,b], Yuxuan Jiang[a,c], Xue Liu[c], Yan Kuai[b], Benli Yu[a,b], Siqi Li[a,b]*

1. School of Physics and Optoelectronic Engineering, Anhui University, Hefei, 230601, Anhui, P. R. China

2. National Key Laboratory of Opto-Electronic Information Acquisition and Protection Technology, Anhui University, Hefei, 230601, Anhui, P. R. China

3. Center of Free Electron Laser & High Magnetic Field, Anhui University, Hefei, 230601, Anhui, P. R. China

#These authors contribute equally.

Corresponding author email: sqli@ahu.edu.cn

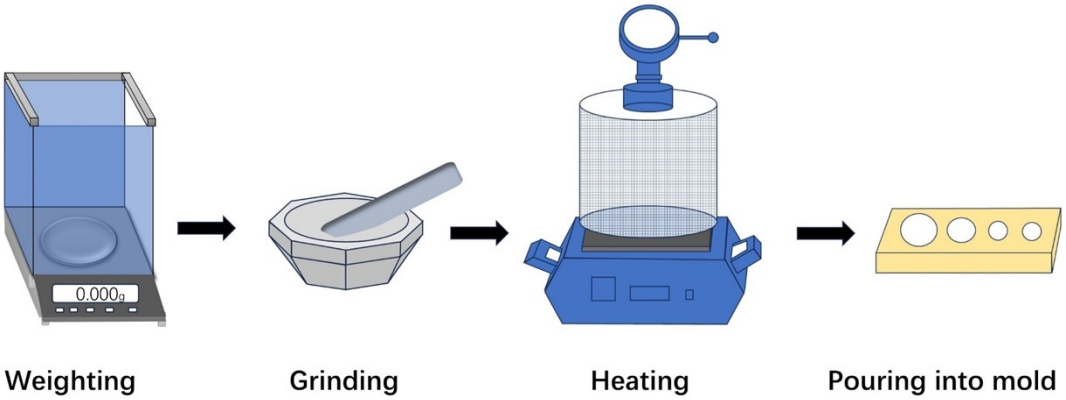

Figure S1 Schematic diagram of the phosphate glass with perovskite precursor fabrication process

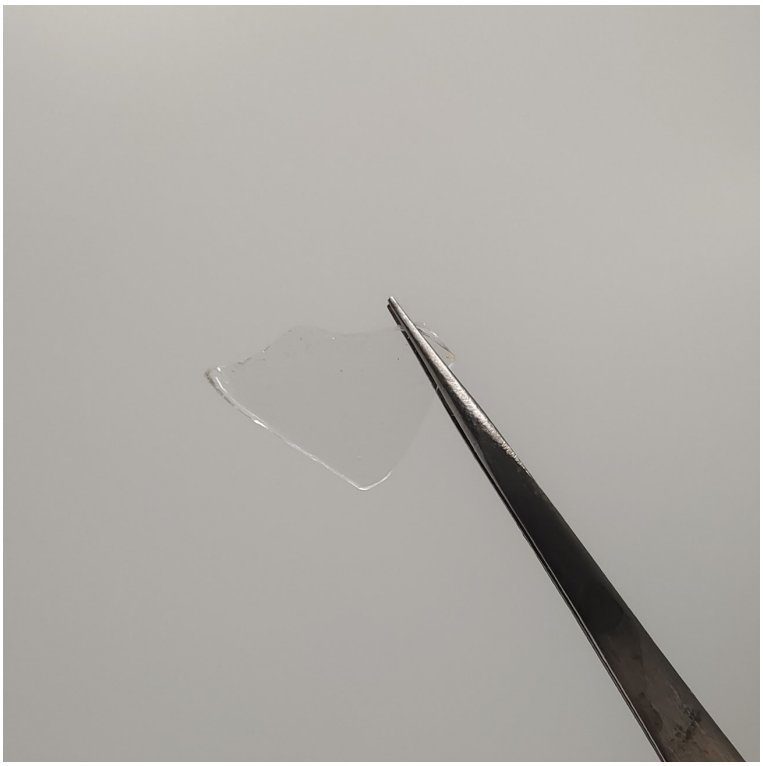

Figure S2 Pristine synthesized transparent perovskite precursors composite phosphate glass.

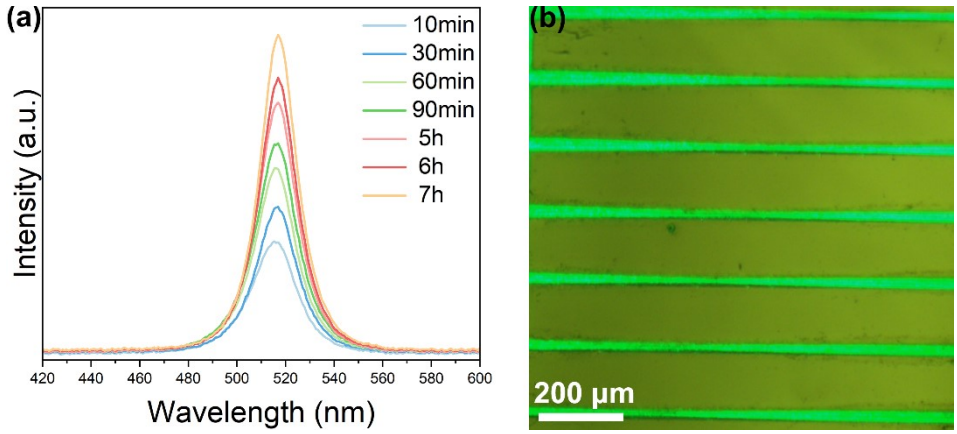

Figure S3 (a) The femtosecond laser is directly written into the formation line of perovskite glass, and the PL intensity curve after 10 min, 30 min, 60 min, 90 min, 5 h, 6 h, and 7 h. (b) Femtosecond laser straight writing on the lines formed by perovskite glass 7 h after photographing under ultraviolet light.

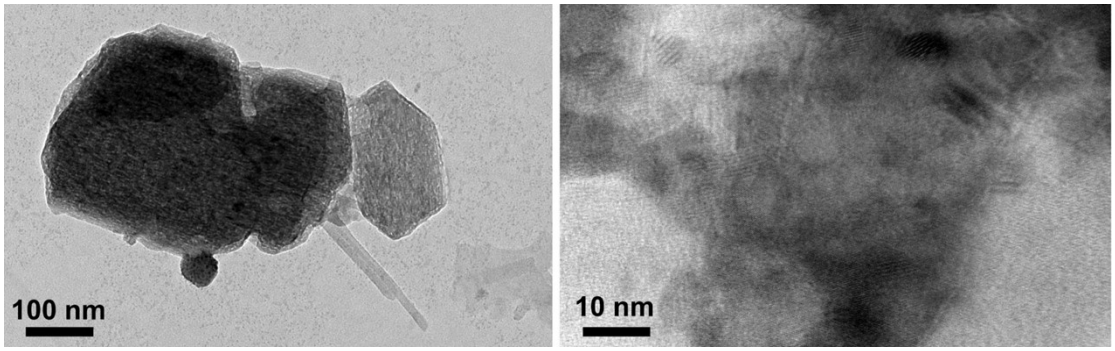

Figure S4 The transmission electron microscope (TEM) images at different resolutions show the structural details of the sample.

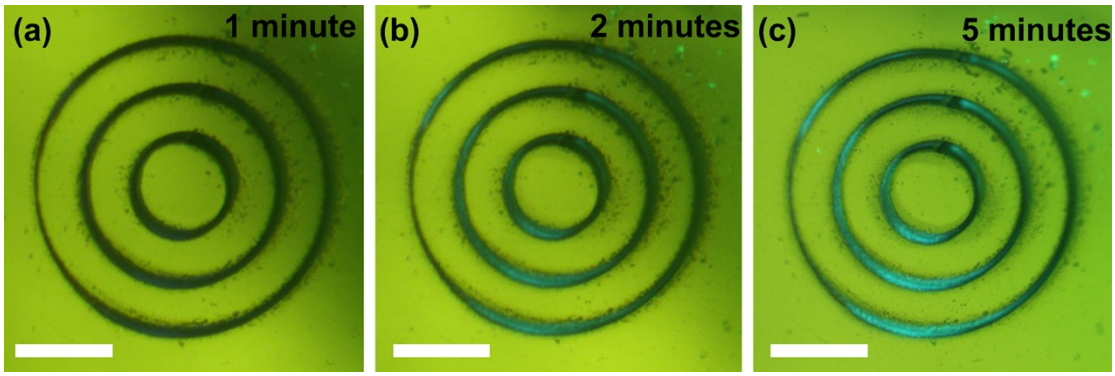

Figure S5 (a-c) Record images of 38.4% perovskite precursor in phosphate glass under 365 nm UV light after fs LDIP technique. The scale bar is 100 μm.

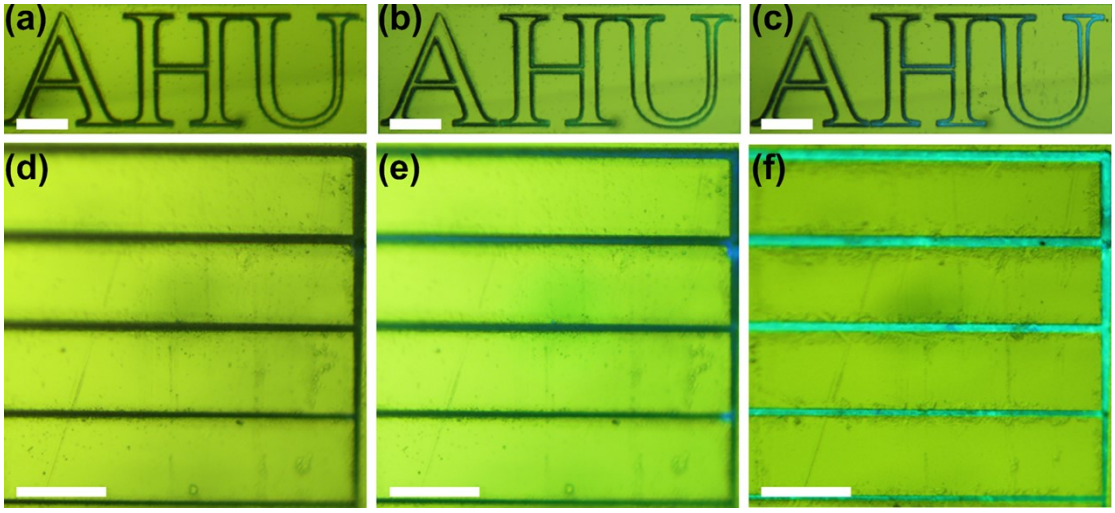

Figure S6 Record images of 23.7% perovskite precursor in phosphate glass under 365 nm UV light (a) after 5 minutes of fs LDIP technique, (b) after heating at 120℃ for 2 h, (c) after heating at 120℃ for 4 h. The scale bar is 100 μm.
(d-f) Record images of 23.7% perovskite precursor in phosphate glass under 365 nm UV light (d) after 5 minutes fs LDIP technique, (e) after heating at 120℃ for 20 minutes, (f) after heating at 120℃ for 1h. The scale bar is 100 μm.

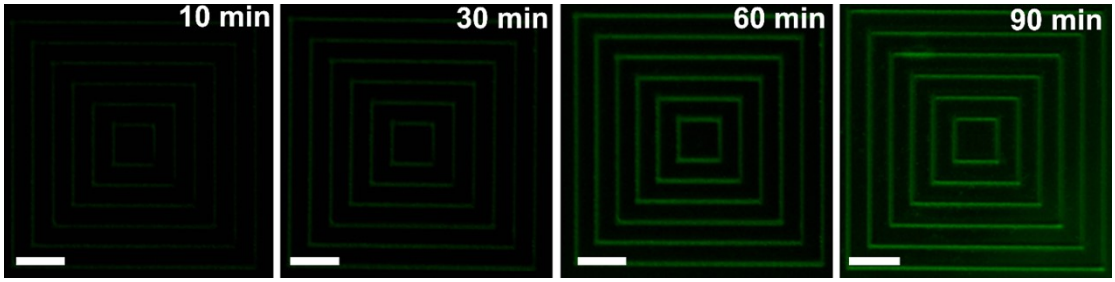

Figure S7 Images of perovskite nanocrystal composite phosphate glass with increased phosphate ratio (15$NaPO_3$-16KPO_3-10ZnO-25/3Al_2O_3-12/5$Al(PO_3)_3$-40H_3BO_3-7Cs_2CO_3-3$PbBr_2$-5NaBr) after femtosecond laser patterning under an ultraviolet lamp at 10, 30, 60, and 90 minutes. The scale bar is 60 μm.

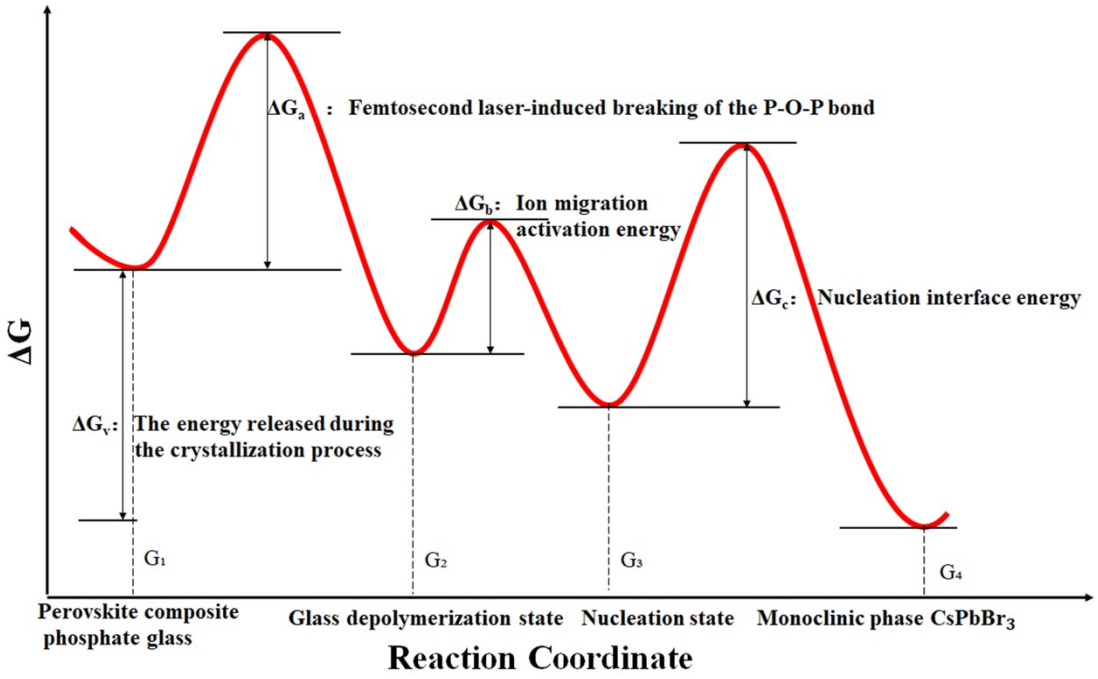

Figure S8 Perovskite growth free energy curve.

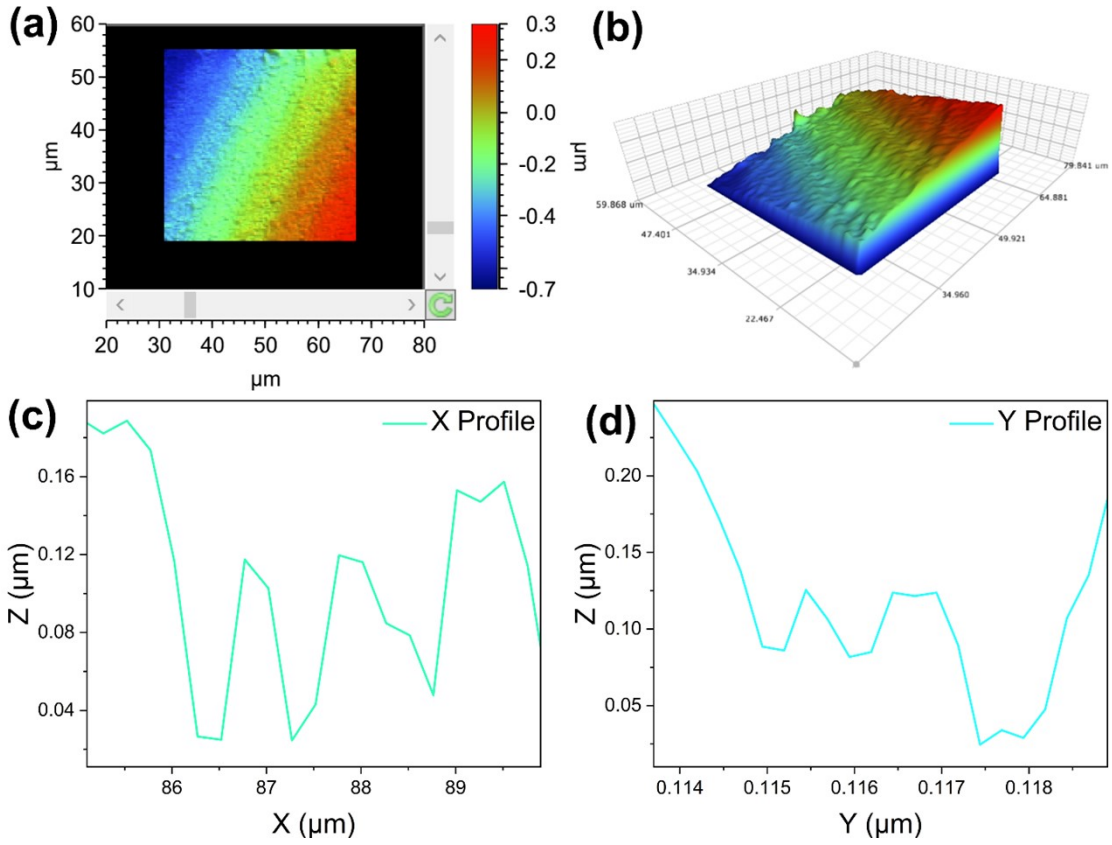

Figure S9 The surface roughness of the pristine perovskite composite phosphate glass.

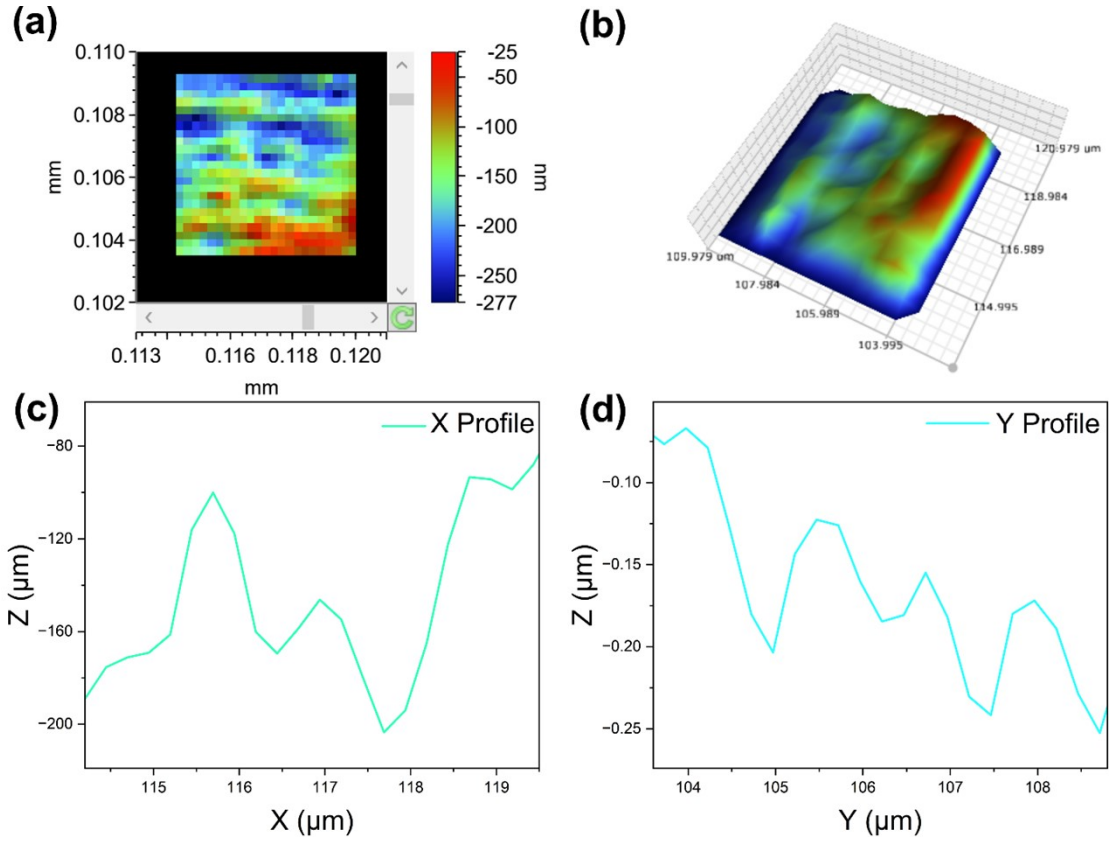

Figure S10 The surface roughness of the 200 μm line patterns.

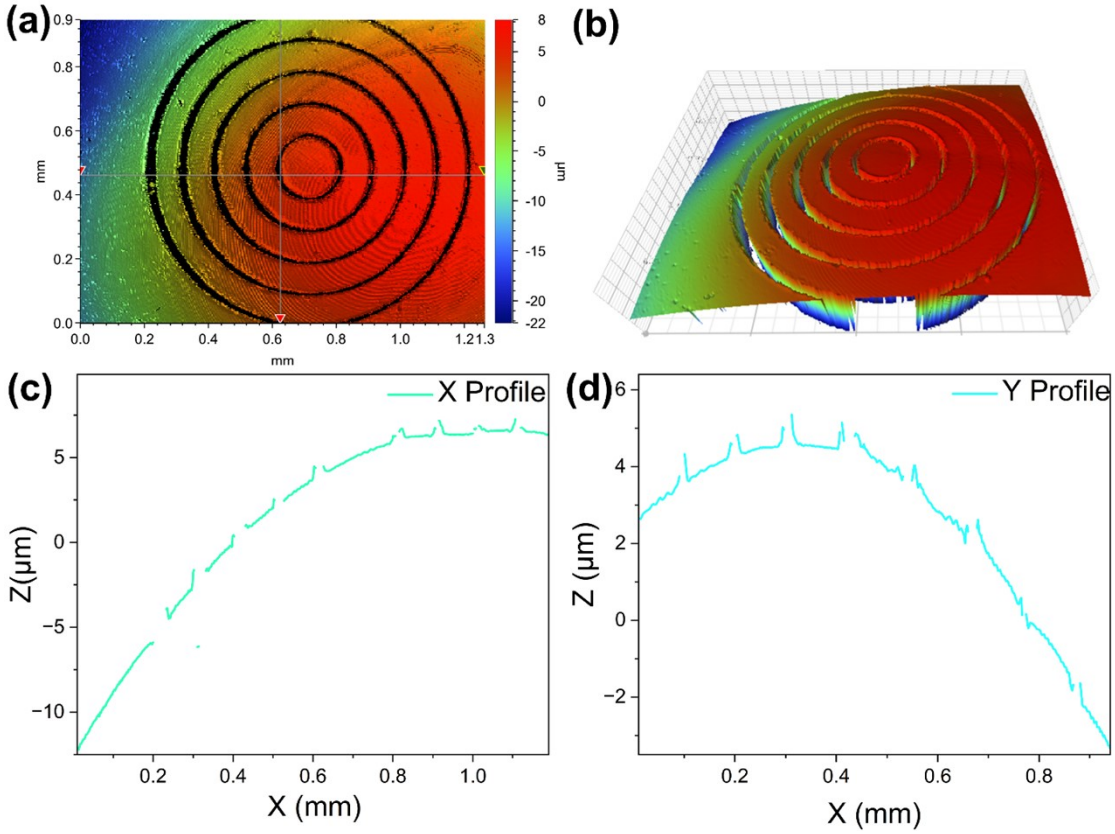

Figure S11 The surface roughness of the 1 mm concentric circles.

Table S1 Statistical summary of parameters for all measured samples.

Parameters / Samples	S_a (nm)	S_q (nm)	S_{ku}	S_p (nm)	S_{sk}	S_v (nm)	S_z (nm)
Primitive glass	16.4	20.4	2.6	55.5	-0.2	-64.6	120.1
200 μm line arrays	42.5	53.4	3.0	147.9	-0.2	-172.2	320.1
Concentric circles	624.8	835.9	9.3	3150.5	-0.8	-12234.9	15385.4

Note: The different surface roughness morphology was characterized by several parameters, including S_a (arithmetic mean height), S_q (root mean square roughness), S_{ku} (steepness), S_p (maximum peak height), S_{sk} (skewness), S_v (maximum valley depth), and S_z (maximum height of surface roughness).

Definitions of surface roughness parameters are provided above.

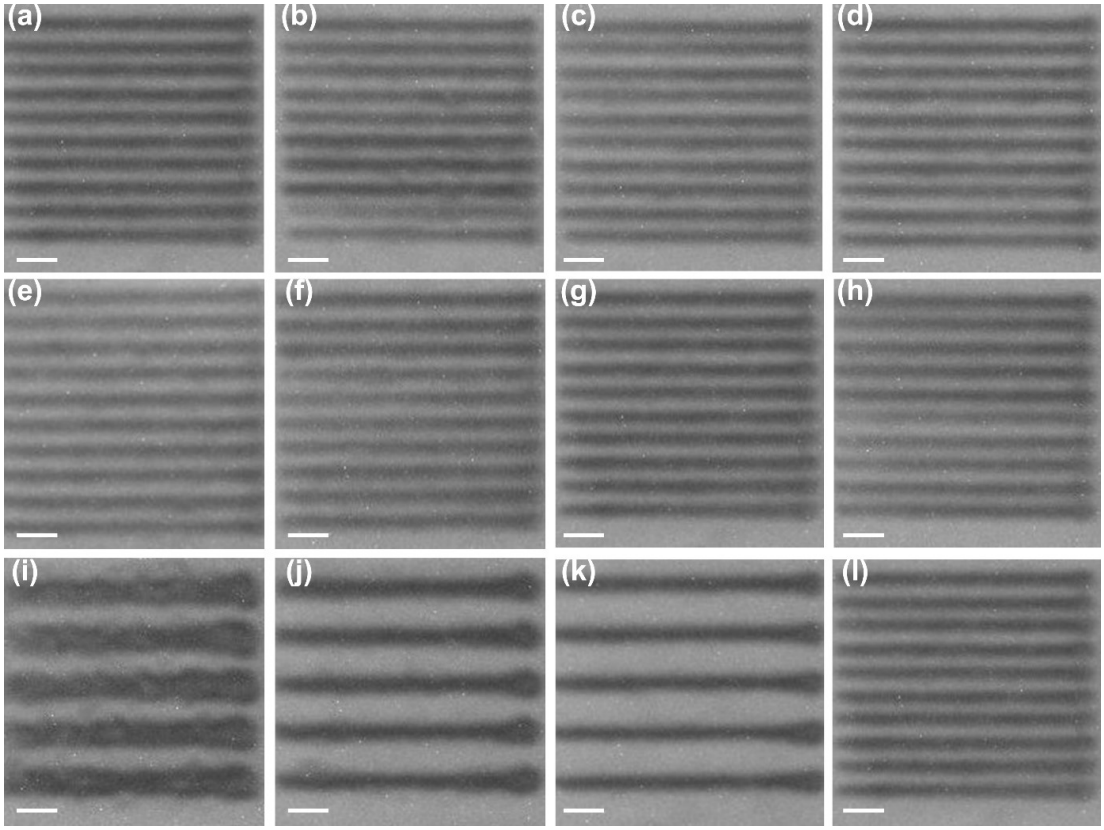

Figure S12 (a-d): Patterns of our method processed at different re-frequencies, respectively 15 kHz, 75 kHz, 250 kHz, and 375 kHz. (e-h): Patterns of our method processed at different speeds, respectively 0.01 mm/s, 0.1 mm/s, 0.25 mm/s, and 0.4 mm/s. (i-l): Patterns of our method processed at different power, 12 mW, 9 mW, 5 mW, and 3 mW. All with a scale of 3 μm.

Table S2. The fabrication accuracy under different femtosecond laser parameters

Re-frequencies (kHz)	Speeds (mm/s)	Power (mW)	Accuracy (μm)
15	0.25	3	0.830
75	0.25	3	0.878
250	0.25	3	0.950
375	0.25	3	1.092
15	0.01	6	1.116
15	0.1	6	1.114
15	0.25	6	1.112
15	0.4	6	1.110
15	0.25	15	2.331
15	0.25	12	1.317
15	0.25	9	1.058
15	0.25	5	1.110

Table S3 Comparison of pattern size and fabrication accuracy with different perovskite pattern strategies.

Materials	Methods	Pattern size	Accuracy	Ref.
$CsPbX_3$	Femtosecond laser-induced forward transfer technique	55×70 μm^2	2 μm	[1]
$(PEA)_2Pbl_4$	Femtosecond laser direct writing technique	1.5×1.5 mm^2	1.78 μm	[2]
$MA_{0.2}Cs_{0.8}PbI_3$ $CsPbBr_3$ $CsPbCl_2Br$	Femtosecond laser processing	15×15 μm^2	3 μm	[3]
$CsPbX_3$	continuous-wave laser-patterning technique	18×24 mm^2	5 μm	[4]
$APbX_3$	hydrophobic/hydrophilic strategy and chemical vapor transport processing	6-inch Si/SiO_2 wafer	2 μm	[5]
$MAPbBr_3$ $MAPbCl_3$ $CsPbBr_3$	droplet-assisted self-alignment approach	10×10 cm^2	200 μm	[6]
$R_2A_{n-1}B_nX_{3n+1}$	Compatible with the photolithography-assisted hydrophobic-hydrophilic patterning process	1×1 cm^2	12.5 μm	[7]
$FA_{0.8}Cs_{0.2}PbI_3$ $CsPbBr_3$ $Cs_{0.75}EA_{0.25}PbBr_3$	Inkjet printing technique	4×7 cm^2	40 μm	[8]
$APbBr_3$ (A=MA, FA, Cs)	Inkjet printing technique	5×5 cm^2	110 μm	[9]
$CsPbX_3$ (X=Br, I, Cl)	Electrohydrodynamic inkjet printing	Diameter of 5 mm	2.8 μm	[10]
$CsPbBr_3$	Femtosecond laser destruction	Diameter of 1 mm	0.83 μm	Our work

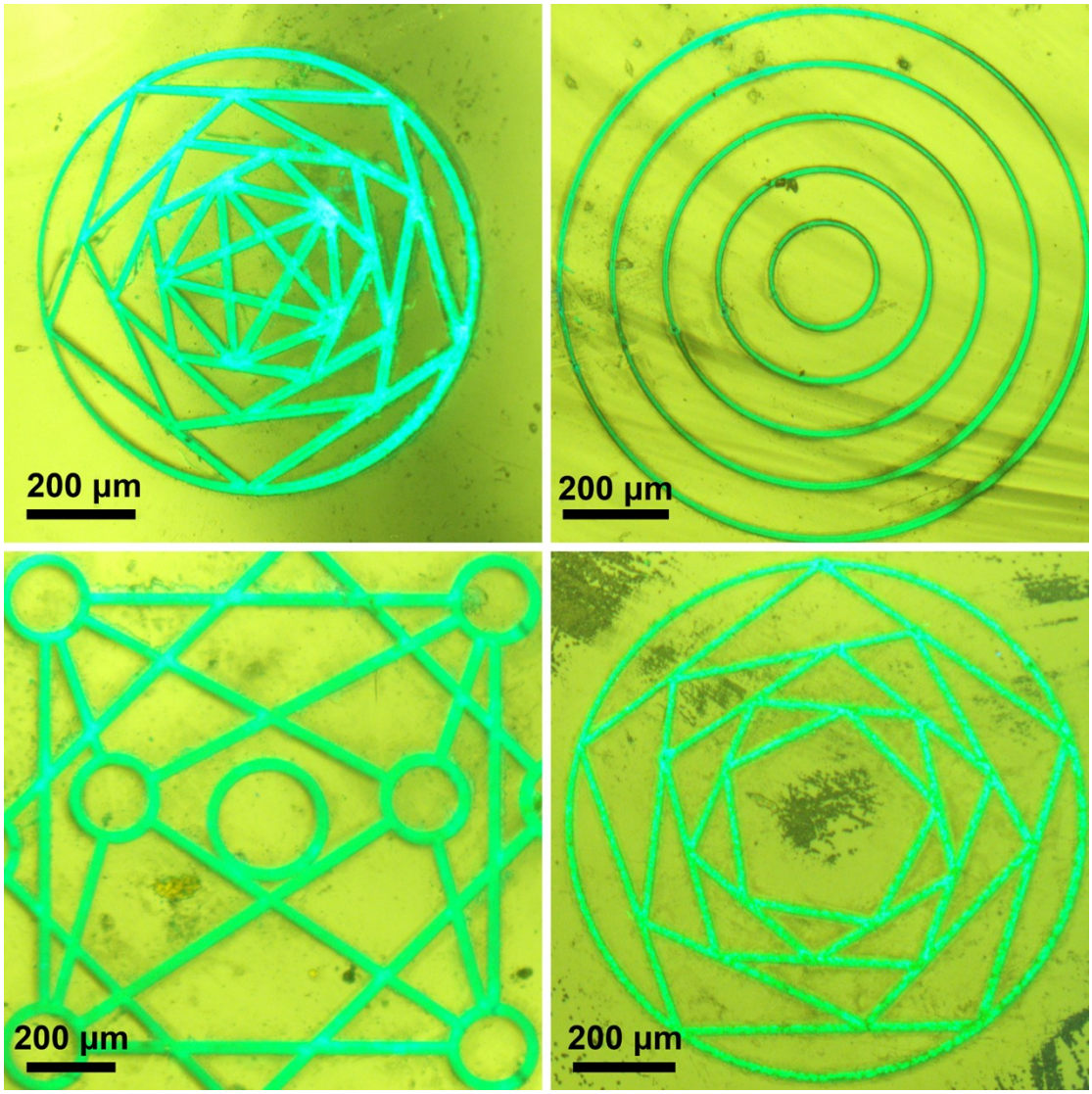

Figure S13 The phosphate glass has been stored for 9 months.

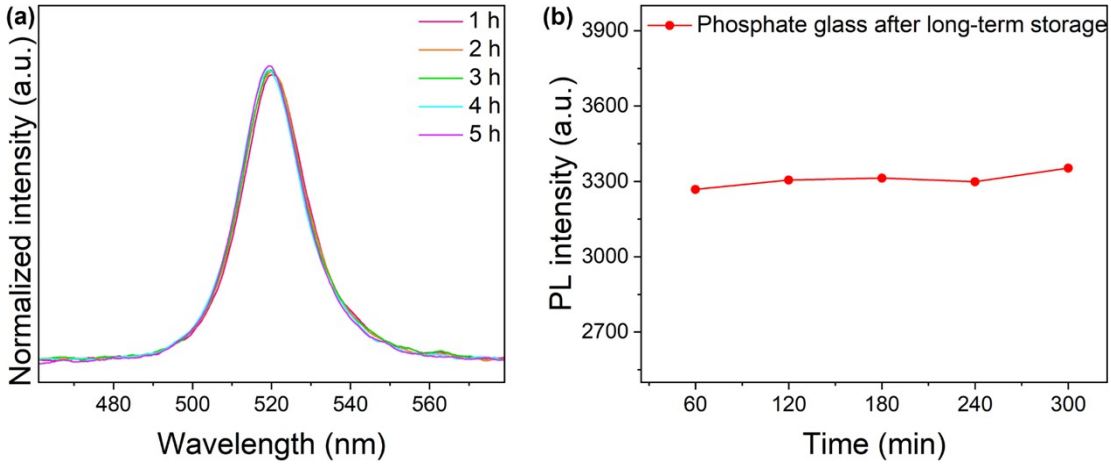

Figure S14 (a) Hourly PL intensity of phosphate glass stored for 9 months during 5 hours of UV irradiation (b) corresponding to the time-dependent PL intensity line graphs.

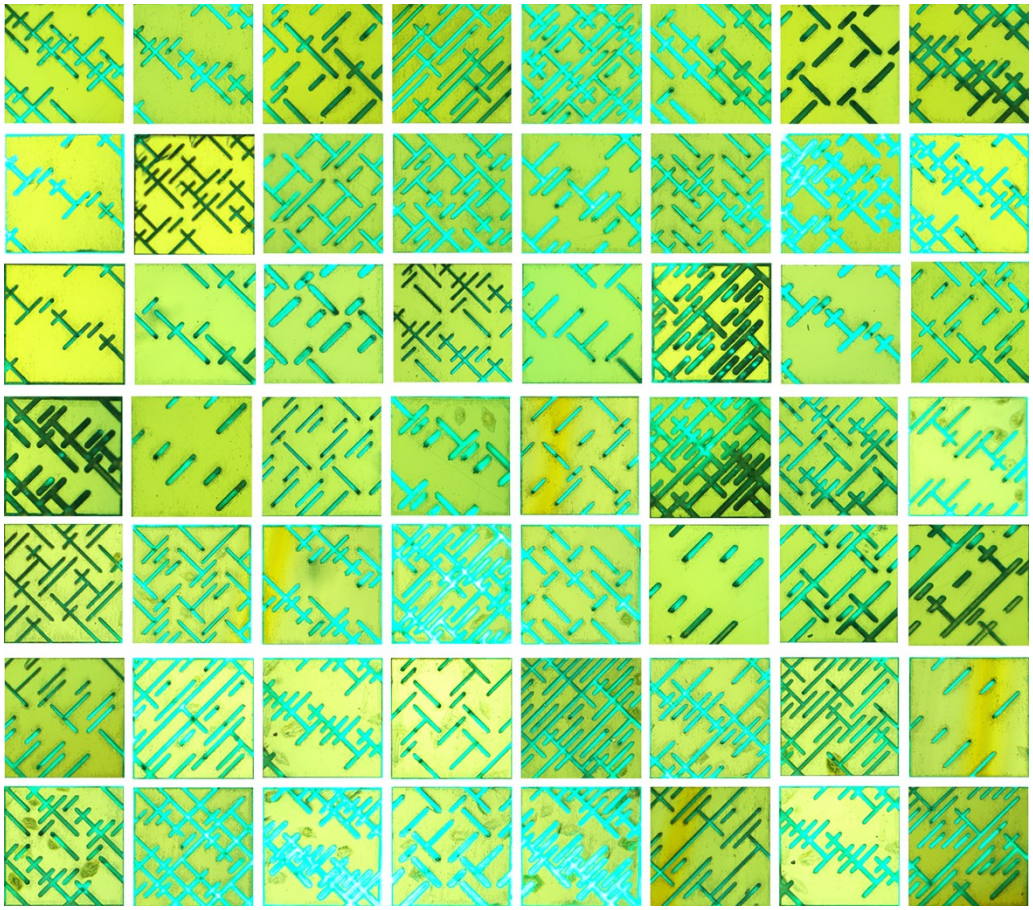

Figure S15 PL luminous pictures after long-term storage, which indicates that the printed pattern can be stored for a long time without being easily damaged, as evidenced by the fact that the processed pattern retains a bright emission after several months.

References

1. S.-Y. Liang, Y.-F. Liu, Z.-K. Ji, S.-Y. Wang, H. Xia and H.-B. Sun, Nano Lett., 2023, 23, 3769-3774.

2. S.-Y. Liang, Y.-F. Liu, S.-Y. Wang, Z.-K. Ji, H. Xia, B.-F. Bai and H.-B. Sun, Adv. Funct. Mater., 2022, 32, 0224957.

3. W. Mao, H. Li, B. Tang, C. Zhang, L. Liu, P. Wang, H. Dong and L. Zhang, Int. J. Extrem. Manuf., 2023, 5, 045001.

4. A. Hu, L. Hou, Y. Yue, S. F. Yu, X. Yu and T. Wang, ACS Nano., 2025, 19, 2286-2293.

6. J. Zhang, Y. Yang, W. Li, Z. Tang, Z. Hu, H. Wei, J. Zhang and B. Yang, Sci. Adv., 2024, 10, eado0873.

7. X. Zhang, Z. Li, E. Hong, T. Yan and X. Fang, Adv. Mater., 2025, 37, 2412014.

8. H. Liu, G. Shi, R. Khan, S. Chu, Z. Huang, T. Shi, H. Sun, Y. Li, H. Zhou, P. Xiao, T. Chen and Z. Xiao, Adv. Mater., 2024, 36, 2309921.

9. L. M. Lifu Shi, Feng Jiang, Yong Ge, Fei Li, Xian-gang Wu, Haizheng Zhong, Adv. Funct. Mater., 2019, 29, 1903648.

10. Y. Chen, X. Yang, X. Fan, A. Kang, X. Kong, G. Chen, C. Zhong, Y. Lu, Y. Fan, X. Hou, T. Wu, Z. Chen, S. Wang and Y. Lin, ACS Appl. Mater. Interfaces 2024, 16, 19, 24908–24919.